

# On-Orbit Operations Simulator for Workload Measurement during Telerobotic Training

Daniel Freer, Yao Guo, Fani Deligianni, Guang-Zhong Yang, *Fellow, IEEE*

**Abstract**—Training for telerobotic systems often makes heavy use of simulated platforms, which ensure safe operation during the learning process. Outer space is one domain in which such a simulated training platform would be useful, as On-Orbit Operations ( $O^3$ ) can be costly, inefficient, or even dangerous if not performed properly. In this paper, we present a new telerobotic training simulator for the Canadarm2 on the International Space Station (ISS), and record physiological data from subjects as they perform a task from the simulator under conditions which increased workload (e.g. latency and time pressure). As most current workload measures are subjective and non-continuous, we analyse how objective measures from the simulator and physiological data can provide a more reliable and continuous measure. ANOVA of task data revealed which simulator-based performance measures could predict the presence of latency and time pressure. Furthermore, EEG classification using a Riemannian classifier and Leave-One-Subject-Out cross-validation showed promising classification performance. EEG results also reveal that Independent Component Analysis (ICA) preprocessing and centrally located channels are more discriminative for 5-class discrimination, whereas information derived from the EEG parietal channels was more accurate in two-class classification of latency and time pressure paradigms.

## I. INTRODUCTION

Telerobotic systems which are directly controlled by a human operator have been utilised in many fields, from surgery [1] to outer space [2]. One of the largest challenges with the use of these systems is the training of novice operators. Various simulators have been created to train surgeons to operate the da Vinci system in different surgical scenarios, and have shown improvements upon traditional methods in some instances [3], [4]. The same is true for some common tasks in outer space [5], but the currently available simulators cannot modulate workload on demand in order to provide different training strategies.

While many groups are investigating ways in which satellites and their robotic components can operate autonomously in outer space [6], teleoperation by humans, manually or in a shared-control mode, will still have a significant role in the On-Orbit Operations ( $O^3$ ) of future spacecraft [7]. Currently, the most successful examples of  $O^3$  come from the International Space Station (ISS), where the Canadarm2 developed by the Canadian Space Agency [8] has taken much of the responsibility for building and maintenance [2].

\*This work was supported by Engineering and Physical Sciences Research Council (EPSRC) under Grant EP/R026092/1.

D. Freer, Y. Guo, F. Deligianni, and G.-Z. Yang are with the Hamlyn Centre, South Kensington Campus, Imperial College London, London, SW7 2AZ, United Kingdom. G.-Z. Yang is also with the Institute of Medical Robotics, Shanghai Jiao Tong University, China.

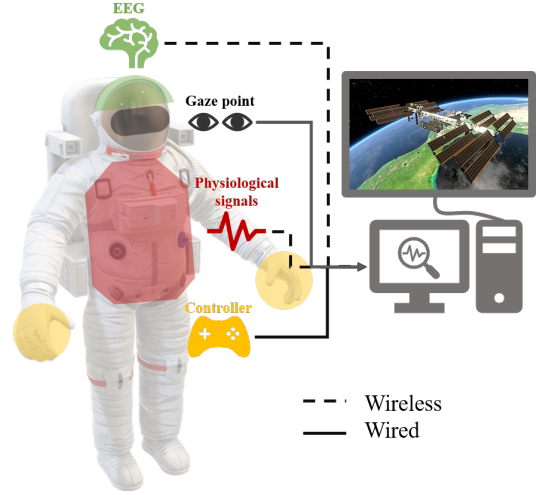


Fig. 1. Wearable technology for physiological signal monitoring of human robot interaction in  $O^3$  tasks.

The Canadarm2 is a complex system, consisting of seven degrees of freedom (DoF), which can be considered as analogous to a human arm (Fig. 2). Three DoF near the base act as the “shoulder” before two long links with a single “elbow” joint between them, with three final DoF that act as a “wrist”. Four cameras are placed on the Canadarm2 at each end-effector and on each of the long links of the arm, and their yaw and pitch can be controlled to provide different views of the task at hand [2].

Aboard the ISS, the Canadarm2 is controlled with the Robotic Workstation (RWS) software, which allows for multiple frames of resolution, control frames, and display frames [2]. As a result, operators of the Canadarm2 must be continuously comparing sensory feedback from multiple sources that can be misaligned. This can lead to increased cognitive load or degraded performance during teleoperated tasks [9]. The visuo-spatial ability of the operator plays an important role in safe task completion, and for this reason, astronauts are required to complete hundreds of hours of intensive training on virtual simulated environments [10].

In this paper, we first propose a photo-realistic simulator for telerobotic training that efficiently modulates workload while simultaneously monitoring multi-modal physiological signals as shown in Fig. 1. Within this framework, we introduce a novel control strategy for complex multi-camera robot manipulation. Furthermore, three realistic confounding factors are introduced to influence both workload and task performance, namely time-pressure, latency and obstacles.

As most current workload measures in this context, such as the NASA-TLX [11], are subjective and non-continuous, we analyse how objective measures from the simulator's subtasks and physiological data can provide a more reliable and continuous measure.

Objective measures of operator performance have been suggested to evaluate the influence of each of these factors on subtask performance in terms of both speed and accuracy. The proposed framework allows us to record physiological signals as they relate to events that are modulated by the virtual world's constraints, but triggered by the user's actions.

In order to verify and study the modulation of mental workload, we additionally analysed the EEG signals of 10 subjects while they performed the task. A Riemannian Minimum Distance to the Mean (MDM) classifier [12], [13] was used to classify short windows of EEG data based on the confounding factors present during task performance. We hope that insights from EEG data will allow for personalised modulation of the training strategy.

## II. CANADARM2 TRAINING SIMULATOR

### A. Canadarm2 On-Orbit Assembly Task

To test the effect of confounding factors on the physiological state of telerobotic operators in training, we have developed a simulator in Unity in which users carry out the capture and addition of a new research module to the ISS. Photo-realistic 3D models of the ISS, research module and Canadarm2 were jointly developed with ZooVFX Ltd. An overview of the task can be seen in Fig. 2. The task consists of several steps:

- 1) Locate the new research module close to the ISS;
- 2) Manually navigate the end-effector of the Canadarm2 to the grapple fixture located on the new research module for secure attachment;
- 3) Navigate the attached research module to its new location, adjacent to the European Space Agency (ESA) Columbus module, avoiding obstacles;
- 4) Dock the module in its desired location.

### B. Control Strategy

In these experiments, the control of the Canadarm2 was achieved using a standard Playstation controller, with each button and joystick indicating the actions shown in Table I. The control methodology was based on the pose of the currently selected camera, with the left joystick movement causing up/down and left/right movement of the robot's end-effector in this camera's coordinate frame. Likewise, using the L2 and R2 buttons moved the end-effector into and out of the screen for the selected camera, respectively. The circle and square buttons turned the last joint of the Canadarm2 for orientation control (roll), while the right joystick similarly turned the yaw and pitch of the end-effector via direct control of the joints. The orientation of the selected camera could similarly be controlled by the D-pad. The cross button closed the latching end-effector of the Canadarm2 around the grapple fixture on the new research module, and the triangle

button unlatched the end-effector and docked the module to its new position, once the desired position was reached.

TABLE I

Controller Button(s)	Action Performed
L1/R1	Select active camera
D-pad	Control active camera orientation
Left Joystick	Move end-effector target up/down/left/right in active camera coordinate frame
L2/R2	Move end-effector target forward/backward in active camera coordinate frame
Cross/Triangle	Connect/disconnect from grapple fixture
Square/Circle	Directly control final joint of robot arm
Right Joystick	Directly control 5th/6th joints of robot arm

Users were able to cycle through which camera was selected by using the R1 and L1 buttons. This change was reflected to the user by drawing a rectangle around the currently selected camera in the user interface. Videos from four cameras were visible to the user during the task, which corresponded to the cameras on the two long links of the robot, the end-effector, and then a camera placed at the desired docking position. Fig. 2 describes the user interface, including the relationship between the camera views and their positions on the Canadarm2.

Inverse Kinematics (IK) of the robot were achieved through iterative gradient descent using the Jacobian, which was constructed using the Denavit–Hartenberg (DH) table of the simulated Canadarm2. The robot continuously updated its joint positions until its end-effector reached within a predefined distance of its target position. Because there was a limit on the angular velocity of each joint, the robot often continued moving after a movement command was finished being given. This gave the appearance of some latency, though additional latency was also added to the system, as described in Section II-C.1. Only the IK of the first 5 links was considered, as any joints past this point were considered to be part of the wrist and could be independently controlled as described above. Dynamics of the robot arm and research module were not considered in this version of the simulator.

### C. Confounding Factors Affecting Space Teleoperation

1) *Latency*: While many  $O^3$  tasks may be performed from a short distance away, for example by an astronaut within the ISS to the Canadarm2, some procedures may also be carried out over a long distance. Ground control often carries out the setup of a Canadarm2 task to save time for the astronauts. In these cases, ground control must cope with between 0.3 and 0.5 seconds of latency, which prevents direct teleoperation. Latency increases with distance, so any teleoperation from ground control to the moon (3-10 seconds) or Mars (20 minutes) would have more issues with latency. Expert users have reported that latency significantly affects their understanding, performance, and efficiency during teleoperated task completion, among other human factors [14].

In our implementation, we considered latency values of 0.5, 1.0, and 1.5 to determine whether different amounts of latency had graded effects on brain function and performance. Latency was achieved by only allowing the control

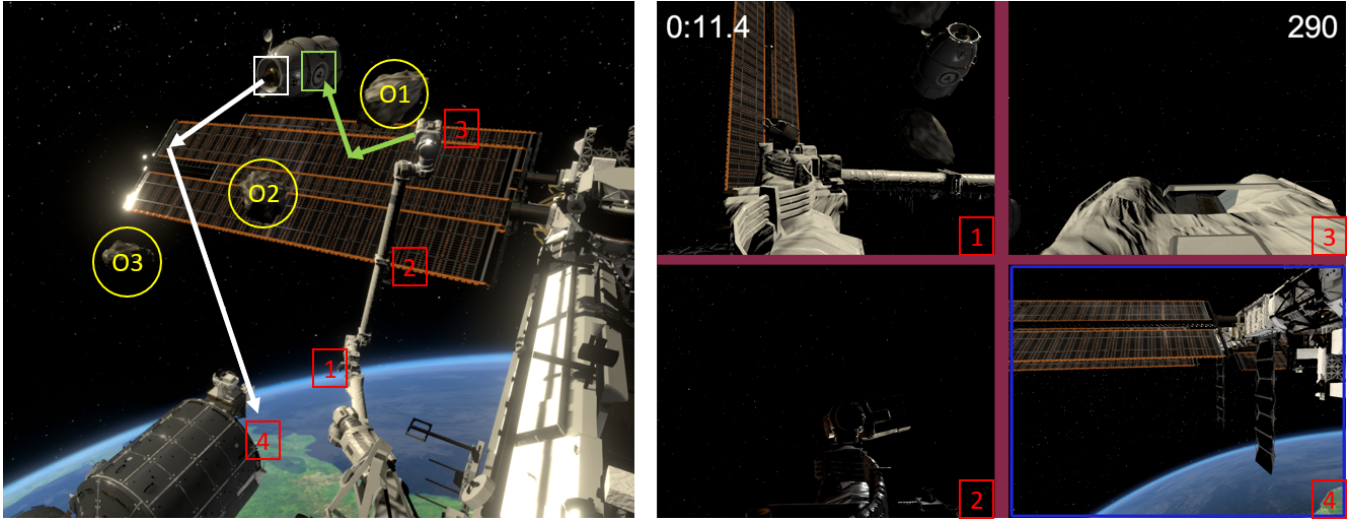


Fig. 2. The description of the task (left) and user interface (right) as shown to users before taking part in this experiment. The left part of the figure shows the two main parts of the task to be completed: 1) Navigate the end-effector to the grapple fixture on the research module and attach (green); 2) Move the research module adjacent to Columbus and dock it there (white). This picture also includes the “debris” obstacles as a confounding factor, labelled as ‘O1’, ‘O2’, and ‘O3’. The locations of four cameras are also indicated with red labelled boxes, and correspond to the similarly labelled views on the right side of the figure. The right side of the figure also shows the timer (top left corner), and scores (top right corner) for a given scenario, and the currently selected camera (camera 4) can be seen surrounded by a blue box.

commands from the controller to take effect once a command’s timestamp was behind the processing time by more than the latency value.

2) *Space Debris*: The presence of debris in space originating from previous missions has become a risk to current and future space missions, causing damage to spacecraft and denying access to certain orbits [15]. While Active Debris Removal missions are crucial to preventing these downsides, consideration of how robots may be operated in the presence of debris or obstacles is additionally a valuable exercise.

To explore this idea, three asteroid-like structures were added into the simulated environment within the workspace of the Canadarm2 to be treated as obstacles for task completion, as debris might be in the future. Any collision of the robot arm or research module with these obstacles resulted in a 100 point decrease in the user’s overall score for that trial. The timings of the initial collision with the obstacles were sent via LabStreamingLayer (LSL)<sup>1</sup> and recorded for comparison with any changes in physiological signals.

3) *Time Pressure*: Astronauts’ time in space is an invaluable resource, with longer missions being associated with serious health effects such as muscle atrophy and effects from radiation. For this reason and because some tasks may have time limitations due to power requirements or other complications,  $O^3$  should be as efficient as possible. Previous research in surgery has shown that adding time pressure has a large effect on the mental state of surgeons during routine laparoscopic tasks [16]. As part of this study we investigate if similar mental changes are seen during this simulated task.

During the experiments, a timer was placed on the screen which counted up toward a time threshold of 4 minutes. The

counting timer turned yellow, then red in color to inform the user that they were approaching task failure. Additionally, the user’s score decreased by 10 points for every 10 seconds of task performance, encouraging speed. Whenever time pressure was added as a confounding factor, the program automatically stopped if the user had not completed the task in time. This often resulted in lower scores, as the final docking of the module increased the score for a given task.

#### D. Performance Measures

Through the completion of the task, users were scored based on their performance. The task starts with the user at 300 points, which decreased 10 points for every 10 seconds the user takes to complete the task, and additionally decreased by 100 points with any obstacle collisions. While time is certainly an important factor to determine operator performance, teleoperated tasks also require precise interactions when the robot is interfacing with other objects. For this reason, at the initial connection to the research module, and at its final docking to the Columbus module, a score related to the quality of the connection was determined and added to the users score. The quality of the grasp was calculated with Equation (1), where  $dist$  is the Euclidean distance between the latching end-effector and the grapple fixture, and  $\theta_{dist}$  is the angular distance in degrees between the same two components. The angular distance was calculated by comparing the quaternion values of the ideal attachment point and the actual attachment point in Unity. For the initial grapple of the research module, the robotic end-effector needed to come within 1 meter of the grapple fixture, while for docking, 3 meters was the distance requirement. There was no strict angular requirement for either step.

<sup>1</sup><https://github.com/scen/labstreaminglayer>

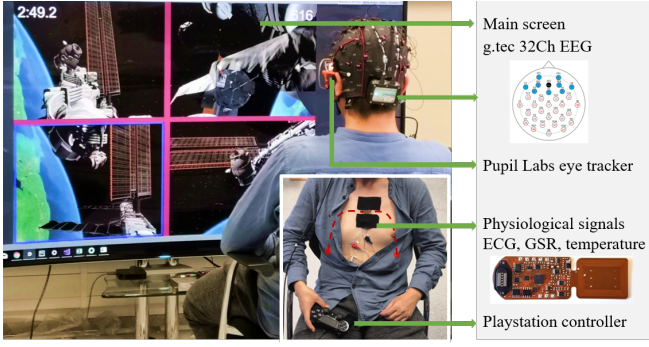


Fig. 3. Experimental Scenario: The subject was asked to finish the simulated teleoperation task with a hand held controller. During task completion, physiological signals were monitored using a g.tec 32-channel EEG cap, a Pupil Labs eye tracking system, and a flexible chest patch acquiring ECG, GSR, skin temperature, and acceleration data. The multi-modal data was synchronised by LSL.

$$Q = 100/(dist + 0.1) + 5000/(\theta_{dist} + 5) \quad (1)$$

### III. DATA COLLECTION

#### A. Experimental Protocol

10 healthy subjects (2 females, 8 males) were asked to complete three blocks of the task while wearing an EEG cap, a PupilLabs eye-tracking system, and a physiological sensor [17] which measured heart rate, galvanic skin response, temperature and body movement. Ethical approval was received (ICREC-18IC4816), and all subjects gave informed consent. While all data was recorded from the subjects during task completion, this paper only provides in-depth analysis of the data sensed from the EEG cap. Some subjects were unable to complete all three blocks due to time constraints or discomfort, so for these cases only the first two blocks were recorded. The three blocks of the task were:

- 1) Familiarisation Block: Users complete the task without any obstacles until they are able to complete the task in under 4 minutes. Then, obstacles are added for one run before moving onto the time pressure block.
- 2) Time Pressure Block (nine total trials): Users complete the task in the presence of obstacles, once with time pressure, once with 0.5 seconds of latency, and once with neither, in a randomised order. This block was completed three times for each subject.
- 3) Latency Block (six total trials): Users complete the task with obstacles and latency. The latencies considered were 0.5, 1.0, and 1.5 seconds, and were assigned in a random order for each subject. This block was completed two times for each subject, with the second time using time pressure as an additional factor.

The signal changes during a typical run through the task can be seen in Fig. 4, which notes several key points during the process, including the initial grapple, a collision, a change in control strategy, final rotation of the module, and docking to finish the task.

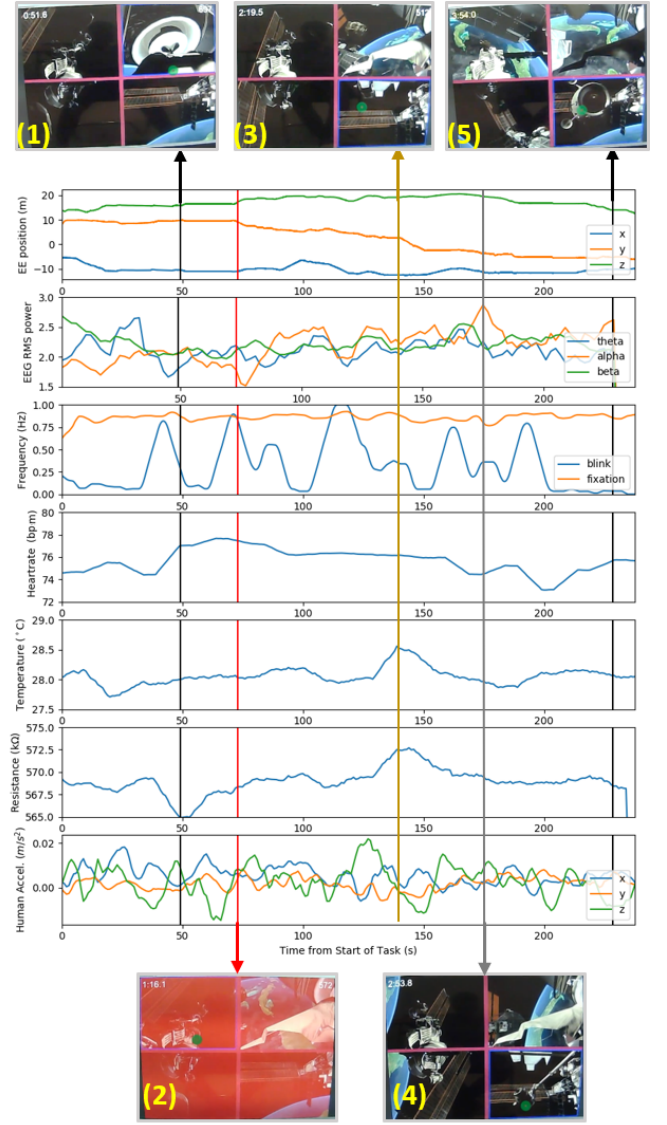


Fig. 4. Multimodal sensor signals and corresponding task images from a typical run through the simulated task. The signals from top to bottom are: End-effector position, EEG frontal lobe RMS power, blink and fixation frequencies, heart rate, temperature, skin resistance (GSR), and the acceleration of the user's body. The highlighted moments from the task include: 1) Grapple 2) Collision 3) Changing control strategy 4) Stop translation and start rotating the component 5) Several seconds before the final docking.

#### B. Brain Signal Collection, Processing, and Classification

Electroencephalography (EEG) signals were captured at 250 Hz through a g.tec g.Nautilus 32-channel wet EEG cap and recorded through Python using LSL. Before recording the impedance of all channels was verified to be less than 30 kΩ. All recorded EEG data were initially notch filtered at 50 and 100 Hz due to electronic noise which was noticed in the Fourier transform of the signals.

After this, three different methods of removing the two known artifacts of eye blinks and muscular (EMG) artifacts were explored. One method of doing this was by using Independent Component Analysis (ICA) using the MNE library [18], considering FP1 as an EOG channel for artifacts removal. The artifacts removed from the signal by



ICA preprocessing include eye-blinks and ECG, while also removing kurtosis and skewness. A second method was to bandpass filter the signal between 2 and 60 Hz using an MNE infinite impulse response (IIR) filter. A third method loosely followed the B-Alert system [19], which has been regarded as one of the best workload classification systems. It utilises a wavelet transform to deconstruct a signal, evaluates and amends the signal based on the deconstruction, then reconstructs it without the higher and lower frequency components. In our implementation, the signal was deconstructed around 6 frequency levels corresponding to approximately 2, 4, 8, 16, 32, and 64 Hz. The signal was then reconstructed without the highest and lowest frequency components. While the original authors additionally normalised data containing eye-blinks and rejected data that contained too much EMG noise, this was not possible for our system. Their method for rejecting eye-blinks relied on a large amount of training data from a similar workload task with many subjects, while we did not have access to such a dataset. Also, in our task muscular movement of the fingers occurs throughout the task, so a high amount of EMG artifacts were often present. Rejecting each of these datapoints would result in too little data, and may also not reflect future training scenarios.

Following this preprocessing, channels were selected in order to reduce the dimensionality of the input signal and ensure that the covariance matrices were Symmetric and Positive Definite (SPD). The same channels were selected for all subjects for a given run and were evaluated experimentally. The different channel combinations tested are shown in Fig. 5, and include a central diamond, central x, frontal, parietal, parallel, and rocket configurations. More channel combinations were additionally considered, but the presented configurations were the most informative in terms of determining which regions were most useful for improving classification performance.

Finally, classification was performed using a Riemannian Minimum Distance to the Mean (MDM) classifier. This method has previously shown promise in the classification of EEG data during motor imagery tasks [12], [13], but has not, to the authors' knowledge, been used for workload classification. Other classifiers, such as linear DFA, were also considered, but tended to fit only to a single class (the non-workload class) due to class imbalance. This problem is not as prevalent in the Riemannian MDM classifier.

Different methods of data processing and classification were evaluated using Leave-One-Subject-Out (LOSO) cross-validation, where the data from 9 of the 10 subjects were used as training data, and the remaining subject's data was used as the test dataset. Data were considered in 2 second non-overlapping windows, and were labelled under three separate paradigms. Under the **5-class paradigm**, labels corresponded to no workload, time pressure, 0.5 seconds of latency, time pressure + 0.5 seconds of latency, and trials with higher latencies (1 or 1.5 seconds). Under the **latency paradigm**, only two classes were considered: those with any amount of added latency, and those without. Similarly, under the **time pressure paradigm**, the two classes considered

were with and without time pressure. For all paradigms, each time window for a given trial was given the same label, despite the fact that some parts of these trials may induce more workload than others. The presented F1 scores were calculated by determining the F1 score for each class for an entire cross-validation run, then averaging these.

## IV. RESULTS

### A. Subject-specific Performance Measures

There was high variability in performance measured across the 10 subjects. Final scores ranged from an average of 15.1 (Subject 1) to an average of 959.83 (Subject 3), while average time to task completion similarly ranged from 351 seconds (Subject 8) to 151 seconds (Subject 4). With 123 total collisions, the most common type of collision was the research module (RM) colliding with the first obstacle (O1), which occurred 55 times. The second most common collision type was the collision of the Canadarm2 (C2) with the body of the ISS, which occurred 29 times. Analysing the reasons for these collisions could help us to develop feedback mechanisms which could prevent them from occurring in a real-life scenario.

### B. One-way ANOVA on Performance Measures

Next, we conducted one-way ANOVA on the performance measures with respect to different simulator-defined factors. As listed in Table II, each element indicates the p-value with and without a specific factor. Here, we mark  $0.005 \leq p \leq 0.05$  and  $p \leq 0.005$  with \* and \*\*, respectively.

It can be observed that the performance measures {Grappling time, Grappling angle, Docking time, Docking angle, Docking score, Duration} show statistically significant differences in the presence of *Obstacles*. With *Latency*, the operators tended to collide more with obstacles, though this was the only significant difference in performance. This is because operators must change their control strategy to compensate for the latency. While the operators were under *Time Pressure*, they finished each  $O^3$  subtask more quickly {Grappling time, Docking time, Duration} than when they were not under time pressure.

TABLE II  
ANOVA RESULTS FOR SIMULATOR-DEFINED PERFORMANCE MEASURES

Variables\Factors	Obstacles	Latency	Time pressure
Grappling time	.000**	.733	.016*
Grappling distance	.244	.139	.285
Grappling angle	.002**	.943	.902
Grappling score	.201	.205	.664
Docking time	.013*	.157	.000**
Docking distance	.195	.675	.741
Docking angle	.001**	.817	.386
Docking score	.046*	.973	.691
Duration	.013*	.157	.001**
No. of Collisions	-	.016*	.285
Final score	.275	.175	.290

\*\* $p \leq .005$ , \* $p \leq .05$

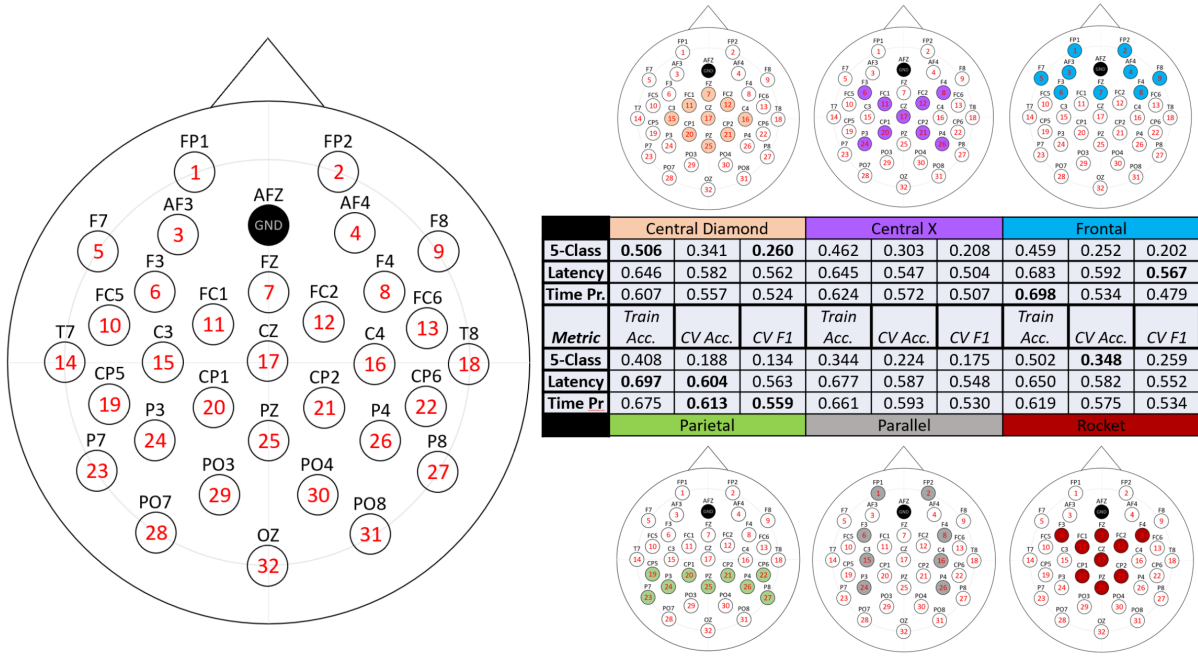


Fig. 5. The layout of the 32-channel EEG cap used for recording and 6 different channel selection configurations considered. Results shown correspond to the accuracy on the training set, the LO SO cross-validation (CV) accuracy, and the LO SO CV average F1 score for a given configuration (channel selection) and paradigm (5-class, latency, or time pressure), using ICA preprocessing.

### C. EEG-based Workload Classification

Results of the channel selection process, as shown in Fig. 5, revealed that the most discriminative channel configurations for the 5-class problem were the central diamond and rocket configurations, which achieved cross-validation (CV) accuracies of 0.341 and 0.348, respectively, with each achieving a CV F1 score of approximately 0.26. The presented results are with ICA preprocessing. As both of these configurations made heavy use of channels near the top and centre of the head, it seems that this region may be the most useful for determining mental workload during training for teleoperated tasks. Any configurations which did not heavily utilise this region did not achieve a CV accuracy of more than 0.252 for the 5-class problem.

However, when considering only the 2-class problems (with or without latency, and with or without time pressure), the most discriminative configuration was with nodes in the parietal region, which achieved among the best CV accuracy and F1 scores for both the latency and time pressure paradigms. Interestingly, this region showed the worst performance in the 5-class problem. The frontal region showed the best performance in terms of CV F1 score for the latency paradigm, but showed the worst performance when discriminating trials with time pressure from those without time pressure, despite having the highest training accuracy.

Using only ICA was determined to be the best noise removal method in terms of the average F1 score in the 5-class paradigm. If considering only CV accuracy, the best noise removal method additionally used the 2-60 Hz bandpass filter, however this filter resulted in more predictions of the non-workload class. Because this class was more prevalent, the

	Central Diamond			Central X			Frontal		
5-Class	0.506	0.341	0.260	0.462	0.303	0.208	0.459	0.252	0.202
Latency	0.646	0.582	0.562	0.645	0.547	0.504	0.683	0.592	0.567
Time Pr.	0.607	0.557	0.524	0.624	0.572	0.507	0.698	0.534	0.479
Metric	Train Acc.	CV Acc.	CV F1	Train Acc.	CV Acc.	CV F1	Train Acc.	CV Acc.	CV F1
5-Class	0.408	0.188	0.134	0.344	0.224	0.175	0.502	0.348	0.259
Latency	0.697	0.604	0.563	0.677	0.587	0.548	0.650	0.582	0.552
Time Pr.	0.675	0.613	0.559	0.661	0.593	0.530	0.619	0.575	0.534
	Parietal			Parallel			Rocket		

TABLE III  
CLASSIFIER PERFORMANCE IN THE CENTRAL DIAMOND AND ROCKET CONFIGURATIONS USING DIFFERENT NOISE REMOVAL STRATEGIES IN THE 5-CLASS PARADIGM

		Train Acc.	CV Acc.	F1 Score
Central Diam.	ICA	<b>0.507</b>	0.341	<b>0.261</b>
	ICA + bp	0.433	0.390	0.167
	ICA + WT	0.416	0.348	0.152
	WT	<b>0.507</b>	0.321	0.238
Rocket	ICA	0.502	0.348	0.259
	ICA + bp	0.434	<b>0.400</b>	0.148
	ICA + WT	0.473	0.262	0.200
	WT	0.394	0.283	0.145

CV accuracy increased, but the F1 score decreased in both the central diamond and rocket configurations. Using the wavelet transform had mixed results, but showed generally poor performance when compared to only using ICA. The only exception to this was when using only the wavelet transform in the central diamond configuration, in which all metrics were fairly good. Both methods of removing higher and lower frequencies from the signal showed worse performance, indicating that features in this frequency range may be indicative of high mental workload.

These accuracies, you may note, are low. However this is reasonable, as some parts of the task require significantly more workload than others. Because we labelled all times within the task as the same workload value, there was likely a large amount of mislabelling in both the training and test sets. This could be improved through better modelling of the task or through consideration of the subtasks which are most associated with mental workload.

## V. DISCUSSION

One criticism of this work may be the fact that much of space research is moving toward autonomy, so research into teleoperation in space will soon be obsolete. However, while the most prominent organisations will likely be able to implement and afford reliable autonomous robotics for space, smaller organisations and companies who are interested in expanding into space may not have this luxury. In addition, new robots and systems may be created for space that are not immediately able to achieve tasks autonomously, so teleoperation could be used to both gather data and gain experience with new robotic systems in space before automation is achieved. Achieving automation is not trivial, which can be seen by the fact that the Canadarm2 is still being teleoperated today, nearly 15 years after its initial use in the ISS. Similarly, some tasks that may need to occur in future space missions, such as surgery, will require intervention from an operator that has specialist knowledge of the situation. This type of task will likely still require teleoperation, as there are significant technical and ethical barriers to autonomous completion of such tasks. In these scenarios, how the confounding factors implemented here affect cognitive load and operator performance will additionally be very important considerations.

Another concern may be the acceptance of this technology by astronauts and other robotic operators. However, many physiological parameters of astronauts (heart rate, oxygen content, etc.) are already measured and monitored during space flight. Whether by their space suits during Extra-Vehicular Activities or for long-term health monitoring, it is logical that future iterations of spacesuits would include more sensors for safety and efficiency. The headsets already used by robot operators in space and on Earth could similarly include technology to monitor brain state during the performance of telerobotic space tasks.

## VI. CONCLUSIONS AND FUTURE WORK

We have proposed a human-robot-interaction framework that modulates workload efficiently and allows for objective performance evaluation and multi-modal bio-signal monitoring. Intended for use during training for telerobotic On-Orbit Operations, this framework additionally considers factors that may be important to such operators such as latency, time pressure, and obstacle avoidance. Additionally, we present results of EEG workload classification with a classifier that had not been previously explored for this purpose. We also provide analysis of different preprocessing methods and channel selection configurations to maximise performance and provide insights into how the brain may be functioning under different conditions.

Future work should focus on combining the information from the various sensors utilised with the framework in order to provide reliable, real-time feedback related to workload which could enhance training protocols. This framework can also be used to study how feedback and semi-autonomous robotic control can affect the workload of operators. We additionally hope to improve the simulator by implementing

multiple types of common On-Orbit Operations, and add realism by conferring with astronauts and other telerobotic operators. Through these improvements, the simulator can personalise and enhance the training of telerobotic operators around, and outside of, the Earth.

## REFERENCES

- [1] W. R. Chitwood, L. W. Nifong, J. E. Elbeery, W. H. Chapman, R. Albrecht, V. Kim, and J. A. Young, "Robotic mitral valve repair: Trapezoidal resection and prosthetic annuloplasty with the da Vinci Surgical System," *Journal of Thoracic and Cardiovascular Surgery*, vol. 120, no. 6, pp. 1171–1172, 2000.
- [2] A. Mishkin, T. Fong, D. L. Akin, N. Currie, and J. Rochlis Zumbado, "Space Telerobotics: Unique Challenges to Human-Robot Collaboration in Space," *Reviews of Human Factors and Ergonomics*, vol. 9, no. 1, pp. 6–56, 2013.
- [3] L. W. Sun, F. Van Meer, J. Schmid, Y. Bailly, A. A. Thakre, and C. K. Yeung, "Advanced da Vinci Surgical System Simulator for Surgeon Training and Operation Planning," *International Journal of Medical Robotics and Computer Assisted Surgery*, no. 3, pp. 245–251, 2007.
- [4] M. A. Lerner, M. Ayalew, W. J. Peine, and C. P. Sundaram, "Does training on a virtual reality robotic simulator improve performance on the da Vinci® surgical system?" *Journal of Endourology*, vol. 24, no. 3, pp. 467–472, 2010.
- [5] K. Belghith, R. Nkambou, F. Kabanza, and L. Hartman, "An intelligent simulator for telerobotics training," *IEEE Transactions on Learning Technologies*, vol. 5, no. 1, pp. 11–19, 2012.
- [6] I. Rekleitis, E. Martin, G. Rouleau, R. L'Archeveque, K. Parsa, and E. Dupuis, "Autonomous Capture of a Tumbling Satellite," *Journal of Field Robotics*, vol. 24, no. 4, pp. 275–296, 2007.
- [7] Y.-k. Zhang, H.-y. Li, R.-x. Huang, and J.-h. Liu, "Shared control on lunar spacecraft teleoperation rendezvous operations with large time delay," *Acta Astronautica*, vol. 137, no. May 2016, pp. 312–319, 2017. [Online]. Available: <http://dx.doi.org/10.1016/j.actaastro.2017.04.014>
- [8] G. Gibbs and S. Sachdev, "Canada and the international space station program: Overview and status," *International Astronautical Federation - 55th International Astronautical Congress 2004*, vol. 11, no. 1, pp. 7405–7415, 2004.
- [9] K. Chintamani, A. Cao, R. D. Ellis, C.-A. Tan, and A. K. Pandya, "An Analysis of Teleoperator Performance in Conditions of Display-Control Misalignments With and Without Movement Cues," *Journal of Cognitive Engineering and Decision Making*, vol. 5, no. 2, pp. 139–155, 2011.
- [10] A. M. Liu, C. M. Oman, R. Galvan, and A. Natapoff, "Predicting space telerobotic operator training performance from human spatial ability assessment," *Acta Astronautica*, vol. 92, no. 1, pp. 38–47, 2013. [Online]. Available: <http://dx.doi.org/10.1016/j.actaastro.2012.04.004>
- [11] S. G. Hart and L. E. Staveland, "Development of NASA-TLX (Task Load Index): Results of Empirical and Theoretical Research," *Advances in Psychology*, vol. 52, no. C, pp. 139–183, 1988.
- [12] D. Freer, F. Deligianni, and G.-Z. Yang, "Adaptive Riemannian BCI for Enhanced Motor Imagery Training Protocols," *2019 IEEE 16th International Conference on Wearable and Implantable Body Sensor Networks (BSN)*, pp. 1–4, 2019.
- [13] A. Barachant, S. Bonnet, M. Congedo, and C. Jutten, "Multiclass Brain-Computer Interface Classification by Riemannian Geometry," *IEEE Transactions on Biomedical Engineering*, vol. 59, no. 4, pp. 920–928, 2012.
- [14] J. Wojtusik, D. Taubert, T. Graber, and K. Nergaard, "Evaluation of Human Factors for Assessing Human-Robot Interaction in Delayed Teleoperation," *Proceedings - 2018 IEEE International Conference on Systems, Man, and Cybernetics, SMC 2018*, pp. 3787–3792, 2018.
- [15] J. C. Liou and N. L. Johnson, "Risks in Space from Orbiting Debris," *Science*, vol. 311, pp. 340–341, 2006.
- [16] H. N. Modi, H. Singh, F. Fiorentino, F. Orihuela-Espina, T. Athanasiou, G.-Z. Yang, A. Darzi, and D. R. Leff, "Association of Residents' Neural Signatures With Stress Resilience During Surgery," *JAMA Surgery*, p. e192552, 2019. [Online]. Available: <https://jamanetwork.com/journals/jamasurgery/fullarticle/2740793>
- [17] B. M. G. Rosa and G. Z. Yang, "A Flexible Wearable Device for Measurement of Cardiac, Electrodermal and Physical Parameters in Mental Healthcare Applications," *IEEE Journal of Biomedical and Health Informatics*, vol. PP, no. c, pp. 1–1, 2019.

- [18] A. Gramfort, M. Luessi, E. Larson, D. A. Engemann, D. Strohmeier, C. Brodbeck, L. Parkkonen, and M. S. Hämäläinen, "MNE software for processing MEG and EEG data," *NeuroImage*, vol. 86, pp. 446–460, 2014.
- [19] C. Berka, D. J. Leventowski, M. N. Lumicao, A. Yau, G. Davis, V. T. Zivkovic, R. E. Olmstead, P. D. Termoulet, and P. L. Craven, "EEG Correlates of Task Engagement and Mental Workload in Vigilance, Learning, and Memory Tasks," *Aviation, Space, and Environmental Medicine*, vol. 78, no. 5, pp. 231–42, 2007.